-RESEARCH PAPER-

International Journal of Mining and Geo-Engineering

IJMGE

IJMGE 59-3 (2025) 237-245

DOI: 10.22059/IJMGE.2025.395329.595250

Electrical imaging of gold-bearing mineralization zones through 3D geophysical modelling

Ali Mohammadi [a], Maysam Abedi [a, *], Mirsaleh Mirmohammadi [a] and Ahmad Zarean [b]

[a] *School of Mining Engineering, College of Engineering, University of Tehran, Tehran, Iran.*

[b] *Civil Engineering Department, Islamic Azad University of Shabestar, Tabriz, Iran.*

Article History:

Received: 14 May 2025.

Revised: 01 June 2025.

Accepted: 07 July 2025.

ABSTRACT

This study illustrates the use of 3D geoelectrical inversion modelling to accurately identify and characterize gold mineralization at a high potential zone in Iran. Nine parallel time domain geo-electrical profiles were acquired using a pole-dipole array, covering a total of 200 meters per profile with 10-meter electrode spacing. The induced polarization and resistivity data were processed and inverted using an unstructured tetrahedral mesh, enhancing the resolution and providing a more precise understanding of subsurface anomalies. The results revealed distinct chargeability and resistivity profiles, which were correlated with siliceous dikes and sulfide-rich zones, both of which are indicative of potential gold mineralization. Shallow anomalies (20-50 meters) align with hornfels layers and display characteristics typical of low-sulfidation epithermal systems, suggesting favorable conditions for gold mineralization. Furthermore, deeper anomalies (50-70 meters), associated with intrusive bodies, exhibit high resistivity and chargeability, consistent with gold-enriched siliceous veins. The study emphasizes the importance of integrating geophysical inversion techniques in gold exploration, as they provide a cost-effective and accurate method for identifying mineralized zones, reducing exploration uncertainties, and enhancing resource estimation. This approach contributes significantly to the efficiency and success of mining ventures by providing valuable insights into subsurface structures.

Keywords: *Electrical resistivity, Electrical chargeability, Inverse modelling, Unstructured meshing, Gold mineralization.*

1. Introduction

Geophysical exploration is a branch of geoscience focused on measuring Earth's physical properties to detect and model subsurface variations. It plays a key role in exploring minerals, oil, and gas. By analyzing data, such as electrical resistivity, density, and chargeability, geophysics helps distinguish mineral- or hydrocarbon-rich rocks from barren ones. Early use of these methods reduces subsurface uncertainty, improves drilling efficiency, and supports better technical and economic decisions in resource development [1].

Geo-electrical methods, especially time domain electrical resistivity and induced polarization (IP), are highly effective for mapping subsurface structures. Widely used in mineral exploration, geotechnical and hydrogeological studies, IP is particularly sensitive to disseminated metallic minerals, such as sulfides, helping to identify high-potential mineralized zones. This reduces geological uncertainties and improves target reliability early in exploration. Data are collected via electrode arrays on the surface or in boreholes, measuring resistivity and chargeability. These depend on factors such as mineralogy, porosity, fluid saturation, and pore fluid types. Analyzing these parameters provides valuable insights into lithology, hydrogeology, and geology for accurate subsurface modelling and resource evaluation [2,3].

Numerical modelling and inversion are vital for interpreting geo-electrical data and analyzing subsurface structures. They reconstruct spatial distributions of parameters, such as resistivity and chargeability, offering high-resolution insights that optimize exploration planning and drilling design. Model reliability is assessed by comparing observed data with computed responses, ensuring consistent and robust subsurface interpretations [4].

Electrical chargeability tomography (induced polarization) has long been used as a near-surface, non-invasive geophysical method for exploring metallic ore deposits. Recently, its use has expanded to engineering and environmental studies. Chargeability is measured in time-domain (TDIP) and frequency-domain (FDIP) modes. FDIP offers richer data and reduces interpretation uncertainties but is costly and time-consuming. Therefore, TDIP is often preferred for rapid and cost-effective exploration [5].

In recent years, the application of geophysical surveys, particularly electrical and electromagnetic methods, has significantly increased in mineral exploration programs due to their potential to reduce both exploration costs and project timelines. The primary objective of these methods, especially electrical techniques such as resistivity and induced polarization, is to identify optimal drill targets that offer high exploration efficiency with minimized financial input. Through the integration of these advanced methodologies, precise spatial delineation of prospective mineralized zones can be achieved, enabling the selection of high-priority targets for subsequent drilling campaigns. This approach contributes directly to the refinement and optimization of exploration strategies, ultimately enhancing operational efficiency and reducing overall project expenditure [6,7]. In the numerical modelling of geo-electrical data, two conventional computational approaches are commonly employed: the Finite Difference Method (FDM) and the Finite Element Method (FEM). Although FDM benefits from a relatively simple mathematical framework, its reliance on structured meshes limits its effectiveness in modelling complex topographies or irregular boundaries. Conversely, FEM, which has seen significant

* Corresponding author: *E-mail address:* maysamabedi@ut.ac.ir (M. Abedi).

advancement in recent decades, supports the use of unstructured meshes, thereby offering superior performance in the simulation of heterogeneous and geologically complex media. In this context, software platforms such as PyGIMLi and ResIPy are recognized as successful implementations of FEM-based modelling, particularly due to their ability to handle unstructured meshing and provide reliable solutions for intricate subsurface geometries [8-10].

Due to the large volume and variability of geophysical data, comprehensive workflows including processing, modelling, and interpretation are necessary. Geophysical modelling is done in 1D, 2D, or 3D, but in complex geological settings, 1D or 2D models are often different from the reality. Thus, 3D modelling is essential, offering better resolution, interpretability, and geological realism, which are crucial for confident exploration decisions [11].

Due to the inherently 3D nature of geological structures, 3D inversion offers the most accurate and consistent interpretation of electrical properties. Although 3D geophysical surveys have become more common recently, their high cost limits their widespread use compared to 2D methods. Advances, such as multi-channel acquisition and powerful computational tools have reduced field time and sped up data processing, increasing interest in 3D inversion. Among electrode arrays, pole–pole, pole–dipole, and dipole–dipole are preferred for their better spatial coverage and data quality [12].

Three-dimensional geo-electrical methods are widely used in geosciences and engineering due to their ability to accurately model complex subsurface structures. They excel in mapping bedrock boundaries by detecting variations in electrical properties and providing high-resolution models. These methods are also crucial for studying subsurface fluid flow by analyzing resistivity and chargeability variations, aiding groundwater and fluid transport understanding. Additionally, 3D geo-electrical techniques support landslide monitoring through detailed modelling of moisture and soil changes, helping predict and manage slope instability in high-risk areas [13-15].

The use of unstructured (triangular) meshing in geo-electrical modelling, especially in mineral exploration, enhances the accuracy and resolution of subsurface structures. Unlike structured rectangular meshes, unstructured grids adapt better to complex geology and topography, allowing optimal node distribution in areas with sharp physical contrasts. This study employed the open-source software ResIPy to compare mesh types under identical conditions. Case studies from Iran, including Talebi et al. (2021) in Atashkouh–Mahallat and a landslide assessment near the Tehran–North Freeway, demonstrated that unstructured meshes provide superior resolution and more accurate delineation of mineralization zones and subsurface details [7, 16].

In geo-electrical data interpretation, inversion transforms raw data into spatial distributions of subsurface electrical properties. ResIPy software provides an intuitive GUI platform to streamline this process, supporting data import, filtering, error modelling, mesh generation, inversion, and visualization. For 2D resistivity, ResIPy uses R2 and cR2 solvers; for 3D, it employs R3t and cR3t engines. Currently, 3D modelling in ResIPy supports only unstructured tetrahedral meshes generated via the Gmsh interface, where each mesh element has four nodes and electrodes are placed at node locations, enabling robust inversions in both simple and complex geological settings [17]. Element sizes are adaptively refined near electrode locations where the potential field is most concentrated, increasing gradually with distance.

This spatial refinement improves modelling accuracy in high-gradient zones, while coarser meshes farther away reduce computational demands. Compared to structured rectangular meshes, unstructured triangular meshes provide advantages in high-resolution geophysical modelling, especially in areas with complex topography. Benefits include fewer inversion parameters, better conformity to terrain variations, and improved detection of subsurface targets with variable shapes [18, 19].

A key advantage of unstructured (triangular or tetrahedral) meshing is the ability to apply localized mesh refinement and assign precise, site-specific physical properties. This is crucial for accurately setting fixed resistivity values or phase angles in targeted model regions, improving the representation of complex subsurface variations. Consequently, unstructured meshing enhances geo-electrical modelling accuracy, especially in heterogeneous and geologically complex settings, leading to more reliable mineral exploration and subsurface characterization [9].

Several studies have successfully applied geo-electrical methods to delineate gold-bearing zones in diverse regions worldwide. Gouet et al. (2012) improved subsurface resolution for gold ore channels in eastern Cameroon. William Guo et al. detected gold-rich siliceous veins in China using resistivity and induced polarization data. Gurin et al. employed time-domain induced polarization to explore gold and silver deposits in Russia, confirming the method's effectiveness in complex settings. In Iran, Malekzadeh Shafavardi et al. investigated porphyry copper–gold mineralization, and Elaminia et al. delineated gold–antimony zones using similar techniques. These works contribute valuable knowledge and methodologies for global gold exploration [23,24].

A major challenge in exploration geophysics is accurately linking geophysical data to geological models, especially in complex gold deposit areas. Advances in electrical resistivity and induced polarization (IP) techniques, combined with multi-dimensional data integration and machine learning, have improved the identification of mineralized zones, enhanced modelling accuracy, reduced drilling costs, and optimized exploration workflows. Continued development of numerical models and algorithms remains essential for clearer gold exploration [25,27].

Gold deposits in Iran are mainly located in two regions: the Sanandaj–Sirjan Zone and the Urumieh–Dokhtar Magmatic Arc. The study area lies near the tectonic boundary between these zones, giving it high mineralization potential. It is situated in northern East Azerbaijan, Varzeghan County, and consists of various sedimentary and volcaniclastic rocks. Geochemical characteristics indicate a low-sulfidation epithermal gold system formed by low-temperature hydrothermal fluids [31].

As shown in Figure 1, a 1:1000-scale geological map outlines the key lithological units and mineralized structures. For this study, a 3D geo-electrical model was constructed using unstructured tetrahedral meshing (Figure 3), calibrated with available drilling data. A strong correlation was observed between geophysical inversion results and other geological and borehole information. Overall, the aim is to develop a more accurate and practical 3D geological model to support gold potential mapping, improve exploration planning, and reduce subsurface uncertainty in future drilling programs.

2. Geological setting

Gold, as one of the rare and highly valuable elements, has formed economically extractable zones and concentrations throughout nearly all geological eras. The earliest evidence of gold accumulation dates back to the Archean Eon, where it became concentrated in specific geological settings such as gold-bearing jaspilites, Banded Iron Formations (BIFs), and stratiform sulfide zones within the sedimentary sequences of ancient greenstone belts [27]. Epithermal gold–silver deposits are typically shallow-seated mineral systems genetically associated with volcanic–hydrothermal environments. They predominantly form along active continental margins and within volcanic arcs related to subduction and extensional tectonic regimes.

These deposits are mainly of the Cenozoic age and are recognized as emerging and economically significant sources of both gold and silver. During the Phanerozoic Eon, epithermal systems became widespread along continental arc settings, with peak development reported in the Mesozoic to Cenozoic, particularly within the Okhotsk–Chukotka volcanic belt and other circum-Pacific regions. Mineralization in these systems is primarily governed by variations in temperature and pressure within hydrothermal fluids and is classically categorized into two end-member types: high-sulfidation and low-sulfidation systems. The former is associated with acidic, non-carbonate-rich fluids, whereas the latter

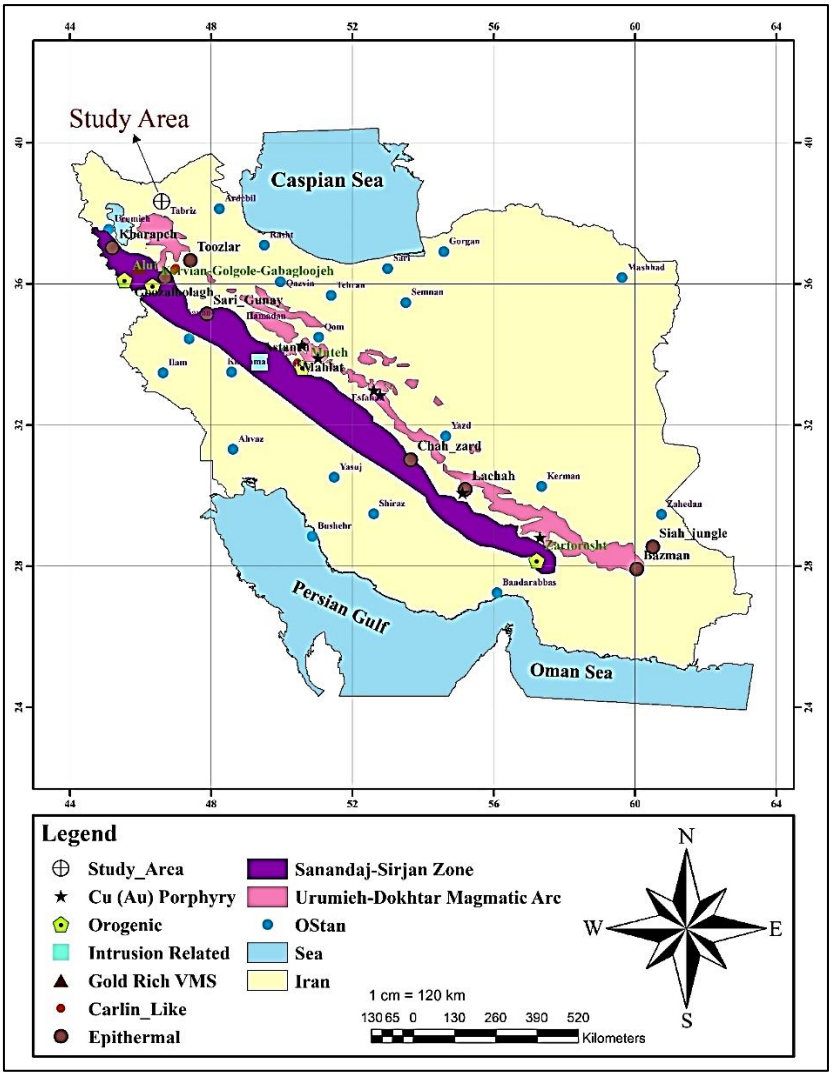

Figure 1. Gold distribution in the Sanandaj-Sirjan zone and Urmia-Dokhtar.

forms from mildly acidic to neutral fluids enriched in carbonate components, both sourced from magmatic–volcanic activity. Collectively, epithermal deposits have played a significant role in precious global metal supply throughout the Phanerozoic and beyond, with their formation closely linked to contemporaneous tectono-magmatic processes [28].

In Iran, gold mineralization is hosted within a wide range of genetic deposit types and metallogenic systems, each reflecting distinct geological and tectonic settings. These include orogenic gold deposits, epithermal systems, Carlin-type analogues, intrusion-related gold systems, and sulfide-hosted gold concentrations associated with volcanogenic environments. Orogenic gold deposits are typically formed under high-pressure and high-temperature conditions in orogenic belts, while epithermal systems develop near the surface in association with volcanic and hydrothermal activity. Carlin-like deposits, more prevalent in arid regions, are generally attributed to shallow-depth sedimentary and hydrothermal processes. Magmatic intrusion-related systems emerge in areas with intense magmatic activity and are often capable of generating large, high-grade gold resources. Furthermore, sulfide-rich volcanic belts, particularly in areas with active or past volcanic history, host economically significant gold-bearing zones. This diversity in gold deposit types not only reflects the complex structural and geological framework of Iran, but also underscores the country's high potential for gold exploration and resource development. Such geodynamic favorability positions Iran as a strategic region in the gold metallogenic province of Western Asia, with the capacity to contribute meaningfully to the global gold supply [29].

The study area is located within the transitional zone between the Urumieh–Dokhtar magmatic arc and the Sanandaj–Sirjan metamorphic zone—two of Iran's most prominent gold-bearing metallogenic belts. These structural domains constitute part of the inner orogenic zone of the Zagros Belt, itself a subdivision of the broader Alpine–Himalayan orogenic system. Gold deposit formation in this region is closely linked to the closure and evolutionary history of the Neo-Tethys Ocean, with various deposit types expected to have developed during different stages of this geodynamic evolution. The presence or absence of specific magmatic intrusions and associated hydrothermal systems plays a critical role in controlling the style, extent, and metal endowment of mineralization across the area. A detailed analysis of the geological context, along with the identification of mineral phases and structural features, is essential for understanding the underlying mineralization mechanisms and assessing the exploration potential of the region. Multiple gold deposit types have been recognized in this area, including stratabound gold mineralization, orogenic gold systems, and magmatic-related deposits. Of particular economic importance are epithermal systems, as well as porphyry Cu–Mo (Au) and Cu–Au deposits, which represent key exploration targets within this metallogenic corridor. Comprehensive investigation of these mineral systems can yield valuable insights into the genetic processes governing gold formation, thereby supporting the development of effective exploration strategies

and resource extraction approaches in this promising region [30].

The exploration area under investigation covers an approximate surface of 20 square kilometers. Field-based geological mapping has revealed the presence of white aplite veins exposed in the southwestern sector of the study area, with a predominant northwest–southeast orientation. The spatial distribution of these veins is illustrated in Figure 4, section (a). Petrographic analysis of thin sections prepared from these veins reveals a predominantly granular texture, accompanied by perthitic structures.

The mineralogical composition is characterized by coarse-grained perthitic feldspar and plagioclase, while the interstitial spaces are largely occupied by quartz and muscovite mica. The textural and mineralogical characteristics described above reflect distinctive crystallization conditions and the geogenic evolution of these veins, suggesting that they may have played a significant role in controlling local mineralization processes.

Further analysis of these veins, particularly in relation to associated alteration patterns and the regional hydrothermal system, can yield critical insights into the genetic model of potential ore deposits in the area [31]. According to the 1:100,000-scale geological map of Varzeghan, the study area encompasses a variety of lithological units, reflecting a complex history of tectonic and sedimentary processes in the region. These units include marly, sandy, and limestone deposits, which were predominantly deposited in shallow marine environments. Their presence indicates relatively stable and low-energy depositional conditions during the early stages of basin evolution. In addition, the widespread occurrence of volcano-sedimentary sequences, tuff, and lapilli tuff of Cretaceous age indicates contemporaneous volcanic activity during sedimentation in this geological period. These units are particularly expressed as rhythmic volcanic–sedimentary layers, reflecting a high degree of basin dynamism during the time of deposition. Intrusive bodies in the area are predominantly composed of quartz diorite and granite and are attributed to the Oligocene epoch.

These intrusions are likely associated with post-collisional magmatic phases related to the closure of the Neo-Tethys Ocean. Given their geochemical composition, tectonic position, and evidence of hydrothermal alteration, these intrusive rocks are considered to play a critical role in the localization of precious metal mineralization. Moreover, scattered Quaternary basaltic outcrops are also observed in parts of the study area. These are interpreted as products of recent volcanic activity, occurring either as extensive lava flows or basaltic scoria cones, and provide important evidence of continued tectono-volcanic processes persisting in the Late Cenozoic [32].

Figure 2 presents the 1:1000-scale geological map of the study area, covering approximately 350 hectares. The map illustrates the stratigraphic sequence of exposed rock units from oldest to youngest, including Cretaceous volcanic rocks (Kv), andesitic lavas (An), rhyolitic tuffs (Kr), and intrusive bodies, such as diorite (Di), syenite (Sy), and alkali granite (Agr). In addition to the Cretaceous formations, Quaternary units identified in the area include basaltic flows (Qb), glacial deposits (Q1), fluvial terraces (Qt1 and Qt2), and alluvial floodplain sediments (Qal).

This stratigraphic framework supports the interpretation of tectonic evolution and the assessment of the mineralization potential of the area. It appears that mineralizing hydrothermal fluids were channeled through fault zones and influenced by semi-deep dioritic and dacitic intrusions, resulting in widespread alteration and the formation of sulfide-rich mineralized zones. Major right-lateral strike-slip faults trending NW–SE, along with subordinate E–W structures, are well developed in the area.

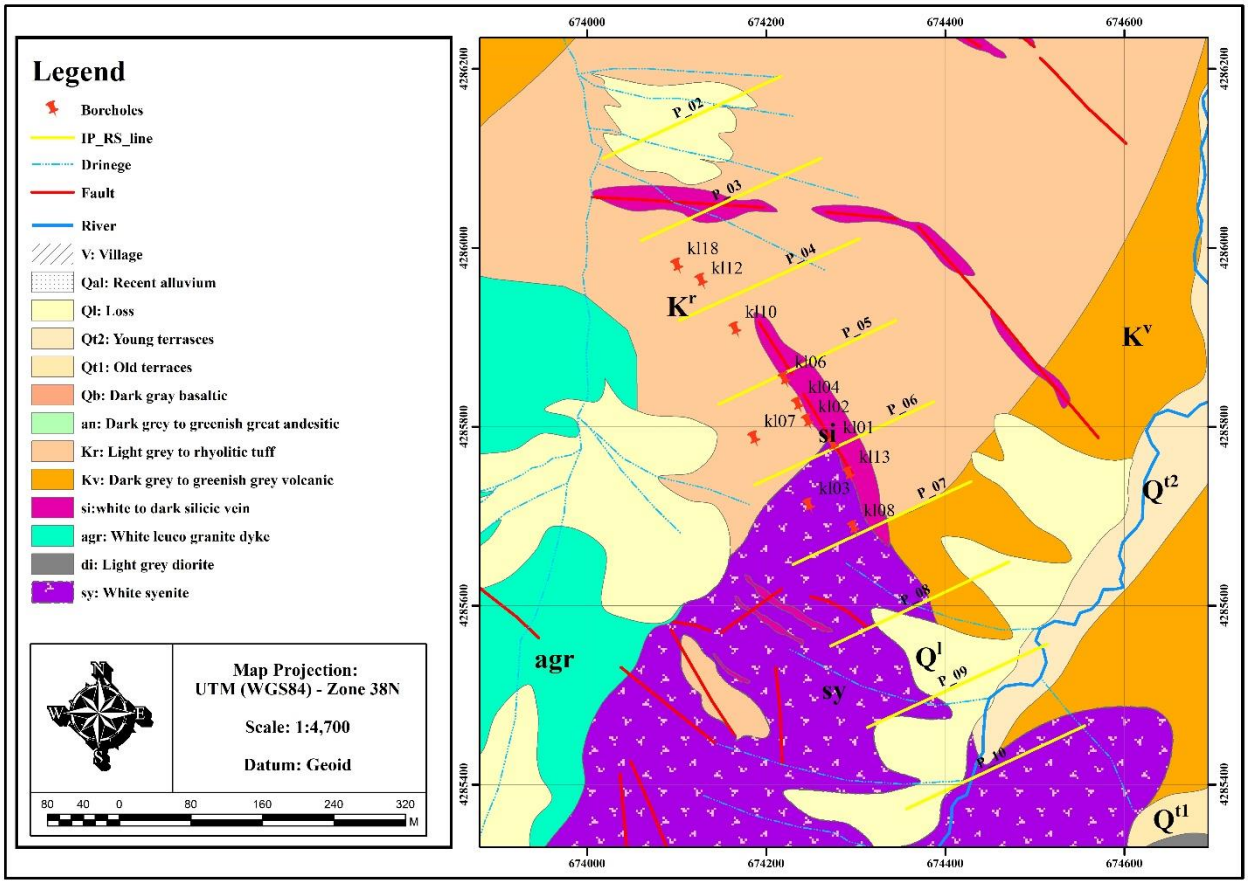

Figure 2. Geological map at a scale of 1:1000 of the study area, along with geoelectric profiles and drilling points.

Associated shear zones have undergone significant hydrothermal alteration and mineralization. A representative E–W fault is illustrated in Figure 4, section (B). Overall, the structural framework, particularly the role of faults in fluid flow, is considered a key control on mineralization within the region [31]. Based on geological investigations and analytical results, the exploration area located in northern East Azerbaijan Province has been identified as a gold mineralized zone characterized by a vein-type mineralization system. The host rocks predominantly consist of rhyodacite and tuff. Thermal studies of mineralization, along with fluid inclusion analyses, indicate that the deposit is consistent with a low-sulfidation epithermal system. In addition to gold, the occurrence of other economically significant elements has also been documented, suggesting that the area possesses enhanced exploration potential for polymetallic mineralization. These findings highlight the strategic importance of the area as a promising multi-element exploration target with favorable geological characteristics and economic viability [31].

3. Geoelectrical survey and data analysis

In this study, a total of nine parallel geo-electrical profiles were acquired in a northeast–southwest orientation to collect resistivity and induced polarization (IP) data. The surveys were conducted using the pole–dipole array configuration, with each profile extending 200 meters, an electrode spacing of 10 meters, and 16 levels of separation per reading. Data acquisition was performed using a 16-channel GDD IP/Resistivity system, manufactured in Canada

Following data acquisition, correction and preprocessing steps were essential to ensure the reliability and accuracy of the interpretation. Raw field data often contain significant levels of noise, and direct interpretation without filtering and modelling may lead to inaccurate or misleading conclusions. In other words, raw measurements alone do not provide a precise image of subsurface structure and behavior. Therefore, establishing a link between field data and the spatial distribution of subsurface physical properties i.e., geophysical modelling is crucial for meaningful interpretation. In the numerical modelling process, the governing physical phenomena are expressed through differential and integral equations. Solving these equations enables the estimation of key subsurface parameters and the reconstruction of the distribution of physical properties within the model, ultimately leading to a more accurate interpretation of subsurface structures. This approach represents a fundamental step in geophysical data analysis, supporting the generation of scientifically robust and interpretable results [33].

Geophysicists have long recognized the importance of data inversion; however, the limited computational resources in the past restricted even the best inversion algorithms to providing only rough estimates for a limited number of parameters. As a result, subsurface structures were often modeled as multilayered systems or simplified prismatic objects, with parameters adjusted to best match the observed data. Given that geological structures typically exhibit complex geometries, such simplifications in numerical inversion modelling often led to erroneous conclusions. In recent years, significant advancements in computational power and inversion mathematics have enabled the development of more realistic inversion models, showcasing the growing importance of geophysics in solving practical geoscientific problems [4].

With advancements in computational technologies, including data processing and digital transmission, geophysical methods are developing at an unprecedented rate. These innovations have made it possible to rapidly and continuously survey vast areas, shifting the focus from limited-scale cross-sectional analysis or local drilling campaigns. The enhanced capabilities of these technologies have expanded their role, allowing for more comprehensive and effective evaluations of geological structures, rather than being confined to detecting specific points [16].

The measurement of time domain electrical resistivity and induced polarization data, as a near-surface geophysical method, provides valuable insights into the chargeability of subsurface materials. This technique is widely used in mineral exploration and engineering studies, such as the identification of bedrock–sediment interfaces, detection of fractured zones, and fault location mapping. Given that nearly all gold mineralization occurs within fractured zones associated with faults and joints, this method has become an effective tool for identifying such structural features. Its ability to generate accurate and reliable data has firmly established it as a key technique in geological and engineering investigations [5, 34]

Geo-electrical methods are based on variations in the distribution of electrical resistivity in subsurface materials. These variations cause changes in electrical responses, which can be measured and analyzed at the Earth's surface. The use of numerical modelling in these methods is considered an essential and indispensable tool, owing to its ability to accurately simulate subsurface phenomena and provide a comprehensive analysis of field data. This approach significantly enhances the quality and precision of data interpretation, facilitating a better understanding of geological features [35].

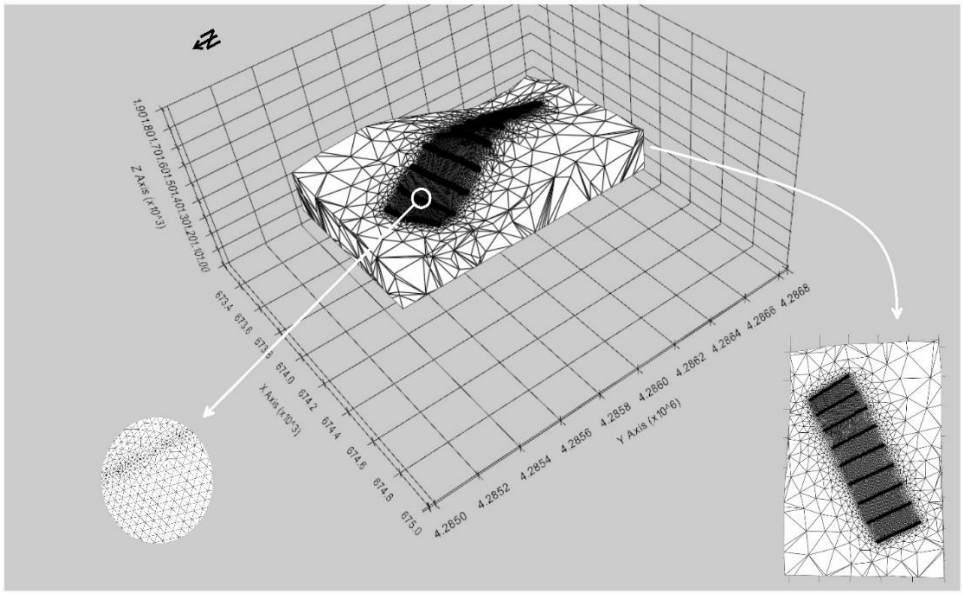

Figure 3. The unstructured mesh considered for subsurface discretization of the physical model domain.

(a) (b)

Figure 4. Outcrop of an aplite dyke (a) and a view of the strike-slip fault surfaces with an east-west trend (b).

The inversion method employed in this study is based on the least squares algorithm. One of the modern and widely used software tools for resistivity and induced polarization studies is ResIPy, which is developed based on this algorithm. The inversion process is utilized due to the complexity of geological structures and the challenges associated with interpreting apparent data. The process continues until the misfit error—defined as the difference between the predicted apparent resistivity from the model and the observed apparent resistivity—is reduced to less than 0.5% to 1%. Once this level of accuracy is achieved, the inversion process is concluded. If the desired accuracy is not reached, the model parameters are adjusted to minimize the error [36].

Unstructured meshing, compared to structured meshing, allows for the representation of the model space with a reduced number of elements, thereby accelerating the inversion process. This approach not only results in time savings but also requires fewer steps to complete the inversion procedure, making it a more efficient modelling technique. This type of meshing is illustrated in Figure 3, showcasing its application [16].

In this region, due to the presence of low-sulfidation gold veins within siliceous dikes and the design of parallel profiles with uniform spacing, it is possible to track anomalies using 3D inversion models for electrical resistivity and IP (Figs. 5 and 6). The behavior of sulfides typically manifests low resistivity and high chargeability in geo-electrical parameters. Additionally, because certain sections of the gold veins are hosted within siliceous dikes, the resistivity in these areas may be elevated. The primary goal of these studies is to track the siliceous dikes, which facilitate the exploration of gold-bearing veins within the study area.

The drilling of 11 exploration boreholes between the profiles has facilitated the examination of geophysical models using core assay data and enabled the identification of significant correlations between them. The locations of these boreholes are shown in Figure 2, with one of the boreholes (KL01) positioned near profile p06, less than 2 meters apart.

Additionally, Figure 7 shows the variation of gold content (a), electrical resistivity (b) and electrical chargeability (c) at borehole KL06, along with its geological column (d). Comparative analysis of these graphs was essential to highlight the correlation between content and geoelectrical parameters.

4. 3D geophysical modelling

As previously mentioned, the study area involved the design and execution of nine parallel geo-electrical profiles using a pole–dipole array. Each profile was 200 meters long, with an electrode spacing of 10 meters and 16 separation points, aimed at tracing the depth of a siliceous dike exposed in the area. Subsequently, 3D inversion modelling of the electrical resistivity and IP data for all nine profiles was performed using an unstructured tetrahedral mesh.

Simultaneously displaying both observed apparent data and the predicted resistivity and chargeability from the inversion models allows for a meaningful comparison of the differences between the two datasets. As is well known, minimal discrepancies between the observed and predicted values are indicative of model accuracy and demonstrate the quality of the inversion modelling process. In Figure 5, the simultaneous display of chargeability and resistivity profiles from both observed data (a,b) and predicted data (c,d) was achieved using an unstructured tetrahedral mesh. To enhance spatial understanding, several sections were generated along the profiles after the 3D inversion modelling of chargeability and electrical resistivity data. In Figure 6a, the inverted resistivity model is presented using the unstructured tetrahedral meshing along the profiles, while in Figure 6b, the inverted electrical resistivity model is similarly displayed along the profiles. As can be seen, the anomalies detected align well with their positions along each profile, exhibiting acceptable repeatability. This suggests the presence of a vertical intrusion-like anomaly consistent with the profile orientations.

The RMS value for the 3D inversion modelling of resistivity and chargeability data was determined to be 1.25 after eight iterations. By comparing the generated models with the geological map of the study area, it is anticipated that these anomalies are associated with siliceous dikes, which are also exposed in the geological map. The possibility of these dikes being mineralized with gold warrants further investigation.

In the 3D model derived from the IP data, areas with moderate to high chargeability (ranging from 15 mV/V to 22 mV/V) were identified, structurally resembling a vein-like system oriented perpendicular to the profiles and coinciding with the siliceous dike exposure in the geological map. Similarly, the 3D model generated from the electrical resistivity data showed that areas with high chargeability correspond to high resistivity values (ranging from 1800 Ohm.m to 2000 Ohm.m). These areas are indicative of the behavior of the siliceous vein (a resistant structure). Additionally, other regions along the profiles were identified, where high chargeability coexists with low resistivity, suggesting that these areas are likely to have a higher concentration of sulfide minerals, independent of gold grade variations.

Gold exploration is inherently complex and challenging due to the intricate geological conditions involved. Accurate interpretation and reliable conclusions regarding gold mineralization zones require high precision and meticulous attention to detail. Analysis of the charts presented in Figure 7 reveals two distinct relationships. The increase in gold grade within the shallow sections (20 to 50 meters depth) coincides with hornfels layers, which exhibit enhanced chargeability alongside uniform but low to moderate resistivity values. Hornfels occurring in epithermal environments typically contain minor amounts of sulfides, and due to their specific mineralogical composition, provide favorable conditions for gold accumulation [37]. It is important to highlight that previous studies have demonstrated a direct influence of the mineralogical composition and sulfide content in hornfels on chargeability and resistivity; these parameters can therefore serve as effective indicators for identifying gold mineralization zones. Furthermore, in certain mining districts, the coexistence of gold and sulfides can cause either an increase or decrease in resistivity, largely depending on sulfide concentration, mineralogical composition, and the

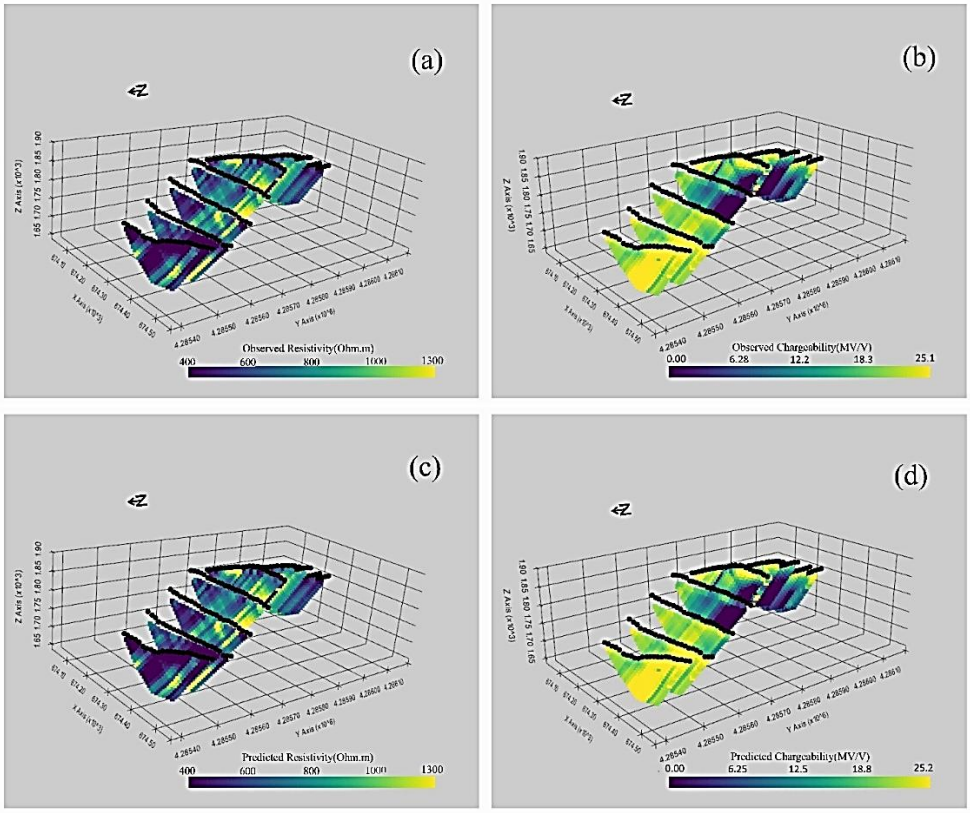

Figure 5. Geoelectrical data surveyed in the area, (a) the observed apparent resistivity data, (b) the observed apparent electrical chargeability data, (c) the predicted electrical resistivity data, and (d) the predicted electrical chargeability data. Data were displayed along nine profiles.

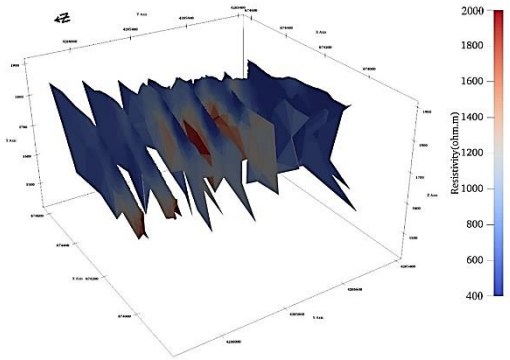

(a)

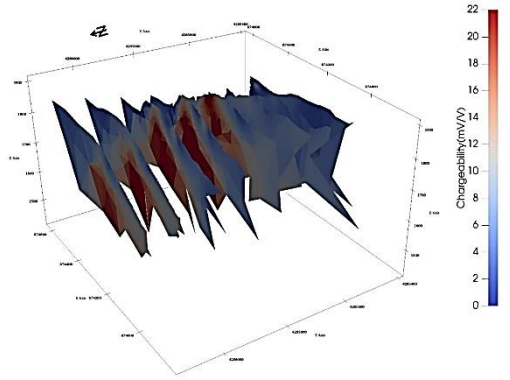

(b)

Figure 6. The ERT models acquired from 3D inverse modeling, (a) electrical resistivity, and (b) electrical chargeability.

average porosity of the host rock (shear grade) [38]. This observation reflects the complex electrical behavior of host rocks in the presence of various minerals and underscores the critical importance of detailed geophysical parameter analysis for more accurate delineation of mineralized zones. However, such behavior has only been partially tracked in some shallow areas. The second, more significant type of gold grade increase reaches its maximum value in the chart and roughly corresponds to an intrusive body located at depths between 50 and 70 meters, characterized by elevated resistivity and chargeability. Given that this section aligns with a siliceous outcrop shown in Figure 7(d), it can be interpreted as a gold-enriched siliceous zone. The correlation of this second type of behavior is notably more distinct within the observable range.

5. Conclusion

This study demonstrates the significant capability of 3D geo-electrical inversion modelling using an unstructured tetrahedral mesh for accurately identifying and characterizing gold mineralization in the study area. The chargeability and resistivity profiles derived from induced polarization (IP) and resistivity data provide valuable insights into the subsurface structure and mineralization potential of the region. The anomalies identified at shallow depths (20 to 50 meters), aligned with hornfels layers, exhibit typical characteristics of low-sulfidation epithermal systems, indicating potential gold accumulation in these zones. These findings are consistent with previous studies on the influence of mineralogical composition and sulfide content on chargeability and resistivity. Furthermore, the deeper anomaly at 50 to 70 meters, associated with an intrusive body, shows features consistent with gold-bearing siliceous veins. This zone, aligned with a siliceous outcrop in Figure 7(d), can be interpreted as a gold-enriched siliceous area. Overall, this study emphasizes the importance of integrating geophysical inversion techniques in gold exploration, as it enables more accurate and cost-effective identification of mineralized zones. By

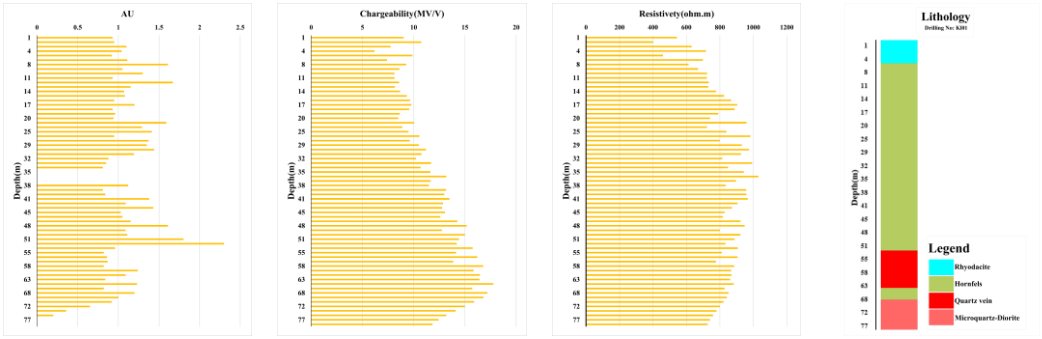

Figure 7. Changes in gold grade (a), electrical resistivity (b), and electrical chargeability (c) at the KL06 borehole location, along with its geological column (d).

providing a clearer understanding of subsurface structures, these methods enhance exploration efficiency, reduce uncertainty, and improve resource estimation, ultimately contributing to greater success in mining projects.

Acknowledgments

The authors would like to express their deep gratitude to Kayhan Zamin Physics Consulting Engineers for providing the data and to the School of Mining Engineering, University of Tehran for all the support provided.

6. References

[1] Gadallah, M.R. and R. Fisher, Seismic Fundamentals, in Exploration Geophysics, M.R. Gadallah and R. Fisher, Editors. 2009, Springer Berlin Heidelberg: Berlin, Heidelberg. p. 17-29.

[2] Dashtbankhor, B., M.K. Hafizi, and F. Jafari, Gold exploration in silica veins in Bajestan County using IP/Rs method, in The Second National Congress of New Technologies of Iran with the Aim of Achieving Sustainable Development. 2015.

[3] Talebi, M.A., et al., Geophysical modeling of resistivity and electrical chargeability data for exploration of building stones, case study: Atashkooh travertine. Applied geophysical research, 2022. 8(1): p. 27-40.

[4] Oldenburg, D. and Y. Li, 5. Inversion for Applied Geophysics: A Tutorial. Near-surface Geophysics, 2005.

[5] Pourhashemi, S., R. Ghanati, and A. AliHeidari, Time-domain induced polarization tomography inversion. International Journal of Mining and Geo-Engineering, 2024. 58(2): p. 153-160.

[6] Mostafaei, K. and H. Ramazi, Application of electrical resistivity method in sodium sulfate deposits exploration, case study: Garmab, Iran. Journal of Biodiversity and Environmental Sciences, 2015. 6: p. 2220-6663.

[7] Talebi, M.A., et al., 3D inverse modeling of electrical resistivity and chargeability data through unstructured meshing, a case study for travertine exploration. International Journal of Mining and Geo-Engineering, 2023. 57(2): p. 131-140.

[8] Rücker, C., T. Günther, and F. Wagner, pyGIMLi: An open-source library for modelling and inversion in geophysics. Computers & Geosciences, 2017. 109: p. 106-123.

[9] Blanchy, G., et al., ResIPy, an intuitive open-source software for complex geoelectrical inversion/modeling. Computers & Geosciences, 2020. 137: p. 104423.

[10] Damavandi, K., et al., Comparison of geoelectric modeling based on structural and non-structural mesh, case study: Tehran-North Expressway, in The Second National Conference on Data Mining in Earth Sciences. 2021.

[11] Ahmadi, R. and J. Ehsan nejad, 3-D geophysical modeling using 2-D acquisitioned data and geostatistics for Yazd, Ali-Abad copper deposit to propose optimal drilling location. Researches in Earth Sciences, 2024. 15(2): p. 77-95.

[12] Loke, M., Tutorial: 2-D and 3-D Electrical Imaging Surveys. 2001.

[13] Chambers, J., et al., Bedrock detection beneath river terrace deposits using three-dimensional electrical resistivity tomography. Geomorphology, 2012. s 177–178: p. 17–25.

[14] Doetsch, J., et al., Imaging and Quantifying Salt-Tracer Transport in a Riparian Groundwater System by Means of 3D ERT Monitoring. Geophysics, 2012. 77: p. B207-B218.

[15] Uhlemann, S., et al., Four-dimensional imaging of moisture dynamics during landslide reactivation. Journal of Geophysical Research: Earth Surface, 2017. 122(1): p. 398-418.

[16] Damavandi, K., et al., Geoelectrical modelling of a landslide surface through an unstructured mesh. Bollettino di Geofisica Teorica ed Applicata, 2022.

[17] Geuzaine, C. and J.-F. Remacle, Gmsh: A 3-D Finite Element Mesh Generator with Built-in Pre- and Post-Processing Facilities. International Journal for Numerical Methods in Engineering, 2009. 79: p. 1309-1331.

[18] Abedi, M., A focused and constrained 2D inversion of potential field geophysical data through Delaunay triangulation, a case study for iron-bearing targeting at the Shavaz deposit in Iran. Physics of The Earth and Planetary Interiors, 2020.

[19] Danaei, K., et al., 3D inversion of gravity data with unstructured mesh and least-squares QR-factorization (LSQR). Journal of Applied Geophysics, 2022. 206.

[20] Gouet, D., et al., Gold Mineralization Channels Identification in the Tindikala-Boutou Area (Eastern-Cameroon) Using Geoelectrical (DC & IP) Methods: A Case Study. International Journal of Geosciences, 2013. 4: p. 643-655.

[21] Guo, W., et al., Geophysical exploration for gold in Gansu Province, China. Exploration Geophysics - EXPLOR GEOPHYS, 1999. 30.

[22] Gurin, G.V., et al., Application of the Debye decomposition approach to analysis of induced-polarization profiling data (Julietta gold-silver deposit, Magadan Region). Russian Geology and Geophysics, 2015. 56(12): p. 1757-1771.

[23] Malekzadeh Shafarudi, A., M.R. Heydarian Shahri, and M.H. Karimpour, Mineralization and geophysical exploration using

IP/RS and ground magnetometry in and around the MA-I area, Maherabad Porphyry Copper-Gold Exploration Area, Eastern Iran. Economic geology, 2010. 1(1): p. 1-17.

[24] Aalaminia , Z., et al., Mineralization and interpretation of geophysical survey, IP/RS, in Hassan Abad Gold-Antimony, northeast of Iran. Iranian Journal of Crystallography and Mineralogy, 2011. 18(4): p. 723-734.

[25] Paterson, N.R. and P.G. Hallof, Geophysical exploration for gold, in Gold metallogeny and exploration, R.P. Foster, Editor. 1991, Springer US: Boston, MA. p. 360-398.

[26] Sono, P., et al., An integrated use of induced polarization and electrical resistivity imaging methods to delineate zones of potential gold mineralization in the Phitshane Molopo area, Southeast Botswana. Journal of African Earth Sciences, 2020. 174.

[27] Ruchkin, G. and Y.N. Deryugin, Zolotonosnost 'rannedokembriiskikh zhelezitykh kvartsitov. Obzor VIEMS Geologiya, metody poiskov i razvedki mestorozhdenii metallicheski poleznykh iskopaemykh, 1988.

[28] Goryachev, N., Gold Deposits in the Earth's History. Geology of Ore Deposits, 2019. 61: p. 495-511.

[29] Aliyari, F., E. Rastad, and M. Mohajjel, Gold Deposits in the Sanandaj–Sirjan Zone: Orogenic Gold Deposits or Intrusion-Related Gold Systems? Resource Geology, 2012. 62.

[30] Heidari, S.M., et al., A review of tectono-magmatic evolution and gold metallogeny in the inner parts of Zagros orogeny: a tectonic model for the major gold deposits, western Iran. Eurasian Mining, 2016: p. 3-20.

[31] Final exploration report of the study area. 2023.

[32] M. Mehrparto, N.K.N., Geological report of the 1:100,000 map of Varzaghan and Kalibar, Geological and Mineral Exploration Organization of the country. 1999.

[33] Farahani, N., et al., Exploration of gold-bearing barite veins using IP and RS methods, in 18th Iranian National Geophysical Congress. 2018.

[34] Park, J.-O., Y.-J. You, and H.J. Kim, Electrical resistivity surveys for gold-bearing veins in the Yongjang mine, Korea. Journal of Geophysics and Engineering, 2009. 6(1): p. 73-81.

[35] Moradzadeh, A. and A. Arab Amiri, Parametric inverse modeling of polarization and resistivity data of a durable mineral index, in The 8th Conference of the Geological Society of Iran. 2009.

[36] Shahmirzae, M. and M. Darijani, Two-dimensional geomagnetic forward modeling using adaptive finite element method and investigation of the topographic effect. Journal of Applied Geophysics, 2014. 105.

[37] Groves, D., et al., Gold Deposits in Metamorphic Belts: Overview of Current Understanding,Outstanding Problems, Future Research, and Exploration Significance. Economic Geology, 2003. 98: p. 1-29.

[38] Seimetz, E.X., et al., Geoelectric Signature of Gold Mineralization in the Alta Floresta Gold Province, Mato Grosso State, Brazil. Minerals, 2023. 13(2): p. 203.